

Drosophila odz Gene Is Required for Multiple Cell Types in the Compound Retina

Yael Kinel-Tahan, Hanna Weiss,[†] Orly Dgany,[‡] Anna Levine, and Ron Wides*

The *Drosophila melanogaster* pair-rule gene *odz* (*odd Oz*, or *Ten-m*) is expressed in distinct patterns in the larval eye imaginal disc. Its earliest eye expression occurs in ommatidial precursors starting from the posterior edge of the morphogenetic furrow. Loss of function of *odz* activity leads to visible light photoreceptor loss; R7 photoreceptor loss; ommatidial size, shape, and rotation defects; ommatidial disorder and fusions; interommatidial bristle defects; and ommatidial lens defects. The same effects are seen in *odz* eye mitotic clones, in *odz-Ten-a* transheterozygous combinations, and in eyes expressing an Odz-Dominant Negative transgene (Odz-DN). Effects of the same strength are also seen when the Odz-DN transgene is driven only in regions of *scabrous* expression, which overlaps the four columns of Odz expression clusters behind the furrow. Small *odz* mitotic clones suggest an *odz* role in cell proliferation or survival. Senseless is expressed in *odz* mutant clones, in a fairly ordered manner, indicating that Odz acts downstream of R8 specification. Disorder within each ommatidium in *odz* clones is accompanied by some loss of R7 precursors and visible photoreceptor precursor order. *Developmental Dynamics* 236: 2541–2554, 2007. © 2007 Wiley-Liss, Inc.

Key words: imaginal disc; Odz/Tenm family; Ten-a

Accepted 22 June 2007

INTRODUCTION

The *Drosophila melanogaster* pair-rule (P-R) gene *odd Oz* (*odz* or *Ten-m*) encodes a membrane-anchored cell surface protein, and not an obvious transcription factor, like other P-R genes (Levine et al., 1994; Baumgartner et al., 1994). *odz* is the archetype of a family of genes found in all metazoans (e.g., Wilson et al., 1994; Wang et al., 1998; Oohashi et al., 1999; Otaki and Firestein, 1999; Rubin et al., 1999; Mieda et al., 1999; Brandau et al., 1999; Ben-Zur et al., 2000), also implicated in pattern formation in development. The first non-*Drosophila* Odz/Tenm mutations,

mouse *Odz4* alleles that lead to failure in gastrulation and somite formation, and a small deletion of the *Caenorhabditis elegans* ortholog that leads to embryo arrest among early defects (Lossie et al., 2005; Drabikowski et al., 2005), support this family's necessity for proper metazoan patterning. Odz/Tenm family members appear to encode receptor like proteins, with discordant yet convergent evidence that discrete domains of the proteins might be processed into elements involved in transcription (Dgany and Wides, 2002; Bagutti et al., 2003; Nunes et al., 2005). These proteins have been modeled, mu-

tually exclusively, as type I and as type II transmembrane proteins, leaving a coherent picture of their mechanism of function enigmatic. Mouse expression evidence verifies that five distinct, partially nonoverlapping, proteins are derived from the *Odz4* locus (Lossie et al., 2005). This variety of protein coding capacity, likely in all members of the gene family, could be the source leading to data supporting two models of the gene products.

Key patterning roles for *odz* in postembryonic *Drosophila* contexts are implicated by expression studies. Odz protein is expressed in the pre-

The Supplementary Material referred to in this article can be found at <http://www.interscience.wiley.com/jpages/1058-8388/suppmat>
The Mina and Everard Goodman Faculty of Life Sciences, Bar-Ilan University, Ramat-Gan, Israel

[†]Dr. Weiss' present address is Immunology Laboratory, Felsenstein Medical Research Center, Petah Tiqva, Israel.

[‡]Dr. Dgany's present address is Pediatric Hematology Laboratory, Felsenstein Medical Research Center, Petah Tiqva, Israel.

*Correspondence to: Ron Wides, The Mina and Everard Goodman Faculty of Life Sciences, Bar-Ilan University, Ramat-Gan, 52900 Israel. E-mail: wides@mail.biu.ac.il

DOI 10.1002/dvdy.21284

Published online 10 August 2007 in Wiley InterScience (www.interscience.wiley.com).

cursors of most *Drosophila* sensory organs, including macrocheatae and chordotonal organs, antennae, and maxillary palps (Levine et al., 1997b). A subset of this expression persists in sensory neurons of the adult. Most intriguing is the Odz distribution in the eye imaginal disc. Odz is expressed in distinguishable ommatidial units in posterior positions of the late larval disc. This late expression persists to the posterior edge of the disc, is point-like in the center of the developing ommatidia, and is lost in *sevenless* mutants (Levine et al., 1997b). Odz is also prominently, but transiently, expressed near the morphogenetic furrow in a dynamic pattern (Levine et al., 1997b). A second *Drosophila* paralog of *odz*, *Ten-a*, for which we have shown a segmentation role (Rakovitsky et al., manuscript submitted for publication), also displays indications of a role in eye development, on which we expand below.

Development of the compound eye of *Drosophila* is one of the most extensively studied models in molecular genetics and development (Tomlinson and Ready, 1987; Pappu and Mardon, 2004). The *Drosophila* retina is composed of a highly ordered array of light sensing subunits termed ommatidia, each with eight photoreceptor cells and additional accessory cells (Ready et al., 1976). The development of this order begins with the differentiation of initially equipotent cells in the wake of the morphogenetic furrow (MF), which traverses the eye imaginal disc from its posterior to anterior side. Behind the MF, clusters of differentiating neurons resolve into a founder neuronal photoreceptor (PR) cell, photoreceptor R8, and subsequent PR cells that are recruited to the ommatidial cluster in an invariant order (Tomlinson and Ready, 1987). The selected presumptive R8 cell must complete its own differentiation, as well as recruit the subsequent seven PR cells and the first of the accessory cells of the ommatidium. Several major signaling pathways are involved in this stochastic process of transforming an undifferentiated epithelial monolayer into an ordered field of subunits of photoreceptors surrounded by accessory cells. These include Decapentaplegic (Dpp, a BMP protein) and Hedgehog in morphogenetic furrow

progression (Voas and Rebay, 2004); Wg in orienting the furrow and eye axes (Lee and Treisman, 2001); Notch, Delta, and Scabrous in initial commitment to a neuronal direction plus subsequent lateral inhibition to regulate placement of ommatidial precursors (Sundaram, 2005); EGF receptor for recruitment of most types of differentiating cells (Freeman, 1998); and the many transcription factors which carry out the gist of the signaling decisions (Pappu and Mardon, 2004). At later stages, the last accessory cells of the ommatidia are dependent on further larval and pupal inductions in the eye disc (Mollereau and Domingos, 2005), to arrive at a complete complement of ommatidial cells. The precise placement of potential Odz activity among these pathways necessitates examining it with respect to these specific processes.

In this work, we have carried out a series of *odz* “knockdown” regimens in the eye to make a first direct assessment of the necessity of Odz for normal retinal development. We achieved this by expressing an Odz-Dominant Negative transgene in the eye; by creating genetically marked *odz*⁻ mitotic eye clones; and by examining the phenotypes of *odz*-*Ten-a* transheterozygous flies. All of the regimens gave the same cluster of phenotypes of roughness, ommatidial disorder, and misallocation of several cell types. *odz* is implicated to act earliest after the furrow, in clusters of developing PRs, then later in proliferation or survival, and in more direct specification of distinct eye cell types.

RESULTS

Odz Is Distinctively Expressed Behind the Eye Morphogenetic Furrow in Ommatidial Precursors

The P-R gene *odd Oz* (*odz*, or *Ten-m*) is strongly expressed in two highly restricted patterns in the monolayer epithelium of the eye disc of the third instar larva of *D. melanogaster* (Levine et al., 1997b). At a late stage of larval retinal organization and development, Odz protein appears in one cell per ommatidium in a *sevenless*-dependent manner (Levine et al., 1997b) and persists (Fig. 1a, arrow-

head, and 1b). At higher resolution and greater sensitivity, this expression proves to be a series of punctate staining patterns adjacent to the R8 cell position (as indicated by nuclear Senseless, see below; Fig. 1l). A vertical section through the disc reveals that this punctate staining is apical of the R8 cell, as expected for R7 (Fig. 1l'). The placement of this apical staining relative to “lower” encircling nuclear staining of visible PRs, and relative to the more basally specifically marked R8 nucleus (aqua), further supports its identification as R7 expression (Fig. 1m).

Preceding this expression considerably, developmentally, is a strong transient appearance of Odz at and posterior to the MF (Fig. 1a, arrow). At higher magnification, this expression strip resolves into discrete blocks of staining aligned in four staggered orderly columns parallel to the MF (Fig. 1b, and magnified inset 1c, arrows). The characteristic morphology of this staining (Fig. 1c) associates it with forming ommatidial clusters of photoreceptor cell precursors “emerging” behind the MF (Tomlinson and Ready, 1987). The cells in each grouping are labeled at their peripheries, consistent with the known plasma membrane localization of Odz protein (Levine et al., 1994; Dgany and Wides, 2002).

The position of Odz-expressing cells near the morphogenetic furrow was clarified by examining double staining for Senseless and Odz protein. This was primarily done with superimposed confocal optical slices, given the different depths of expression of these two proteins within the disc (Fig. 1d-h, h'). Senseless expression, first appearing in the furrow in intermediate groups, becomes restricted to two to three cells migrating apically, the R8 equivalence group (Fig. 1e; Frankfort et al., 2001). Senseless expression is subsequently further restricted to the single R8 precursor cell per forming ommatidium, then to R8 cells (Fig. 1e). The anterior-most Odz expressing clusters are just posterior to the R8 equivalence groups (Fig. 1d-f). At higher resolution, juxtaposition of the earliest expression of Odz and Senseless indicates that Odz is expressed in the ommatidial precursors containing the first singlet R8 precursors, column

0 (Fig. 1g; see Tomlinson and Ready, 1987; Wolff and Ready, 1993; Jarman et al., 1995; Baker and Zitron, 1995). The Odz expression clusters are each associated around one R8 Senseless-expressing cell that lies in a deeper focal plane in the disc (Fig. 1h). A vertical cross-section through these discs in column 0 (between two arrows in Fig. 1h), show Odz protein expressed apically, above each associated R8 cell (Fig. 1h').

In column 0, Odz is expressed peripherally in up to eight cells, whereas by column 3, often just two cells display expression (Fig. 1c,g,j,k). Morphologies of Odz staining clusters derive from expression within a subset of the cells whose apical membranes are known to stain darkly with cobalt sulfide (Tomlinson and Ready, 1987). Column 0 displays membranous Odz expression on a portion of "rosette" formations, column 1 shows "arc" morphologies, and columns 2 and 3 appear as wholly or partially stained (respectively) closed preclusters (Fig. 1j,k). Rosettes are primarily stained only on their posterior half (Fig. 1j, arrow). The most posterior Odz expression, in column 3, appears only in prospective R3 and R4 cells (Fig. 1k, arrowheads). The column-wise expression placement was bolstered by performing double staining of eye discs for Odz and Elav proteins (Fig. 1i). Elav, known to be weakly detected most anteriorly in R2 and R5 in column two (Yang and Baker, 2006), is seen to partially overlap the Odz-expressing rows. Elav overlaps the fourth, or third and fourth, column of Odz expression (columns 2 and 3). Overall these data support a transient expression pattern of Odz in the wake of R8 specification, when the first additional photoreceptors are being recruited.

Carboxy-Terminal Truncated Variant of the Odz Protein Exhibits Dominant Negative Odz Activity

Odz protein bears EGF-like repeats that are most similar to those of the *Drosophila* proteins (Levine et al., 1994; Adams et al., 2000) Notch and its ligands Serrate and Delta, as well as the Notch modulator Crumbs (Herranz et al., 2006). We have examined the Odz protein using a battery of antibodies, and model the protein as a

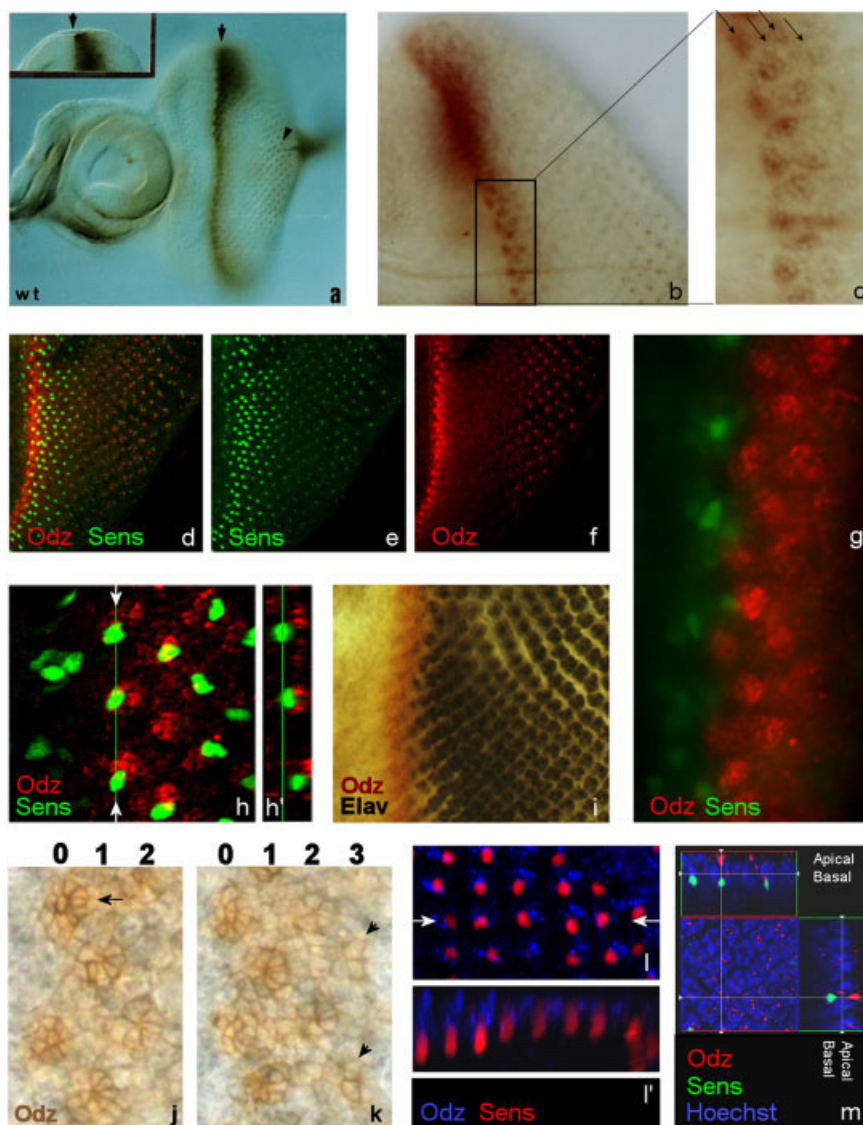


Fig. 1. Odz is expressed behind the morphogenetic furrow (MF) of the eye imaginal disc. All eye discs are oriented with the posterior to the right, anterior to the left. **a–c:** Immunocytochemistry based on anti-Odz monoclonal mouse antibody followed by horseradish peroxidase (HRP)-conjugated secondary antibody and diaminobenzamide (DAB) turnover (brown). **a:** Odz is expressed posterior to the morphogenetic furrow (arrow) and as point-like expression in more mature developing ommatidia (arrowhead). **b:** At higher magnification, Odz can be seen in four staggered columns of preclusters after the furrow. **c:** At higher resolution, Odz can be seen at the periphery of cells in the four columns (arrows) of the clusters. **d–f:** Odz (red immunofluorescence, f), Senseless (green immunofluorescence, e), and both expressions merged (d), in a confocal image showing overlapping sections from a wild-type third larval eye disc. The Senseless image is from a confocal optical section deeper in the eye disc than that of Odz. **g:** A higher resolution view of Odz (red) and Senseless (green) expression along the MF. **h:** Odz and Senseless expression in R8 equivalence groups and in columns 0–3. **h':** A vertical cross-section through the disc examined along the line demarcated by white arrows in h. Apical is on the right. **i:** Rat anti-Elav antibody covisualized, using anti-rat horseradish peroxidase (HRP) secondary and diaminobenzamide (DAB) turnover in the presence of Cobalt (black), with anti-mouse HRP Odz standard immunocytochemical staining (brown). **j:** High resolution view of Odz (HRP) in ommatidia at the furrow. The three most anterior columns of Odz-expressing cells (marked columns 0–2) are in "rosette" (0), "arc" (1), or closed precluster (2) groupings. Odz only stains a portion of the rosette (arrow). **k:** Odz (HRP) as in j with the four Odz expressing columns (marked columns 0–3). The column 3 closed preclusters (arrowheads) are stained only in their most anterior cells, prospective R3 and R4 precursors. **l:** A high resolution view of Odz (blue) and Senseless (red) in the region of developing R7 cells, with a cross-section through the disc examined along the line demarcated by white arrows, as displayed in h'. **l':** apical is up, basal is down. **m:** A-high resolution view of Odz (red), Senseless (green), and Hoechst nuclear staining (blue) in the region of developing R7 cells. Cross-sections through the disc examined along the lines demarcated by white arrowheads in an X and Y axis are shown above and to the right, respectively. They show apical Odz staining in red, nuclei of the cells in clusters in blue, and the basal R8 nucleus in aqua (green and blue together).

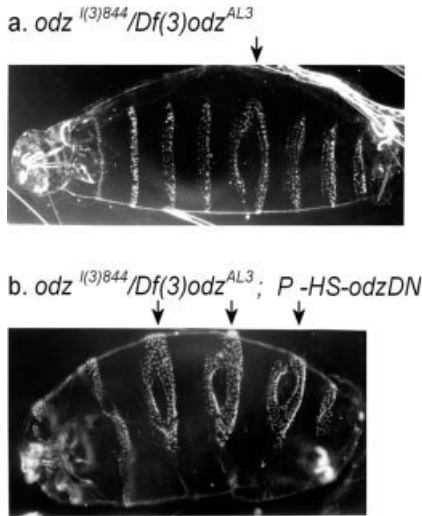


Fig. 2. A C-terminal truncation transgene confers Odz-Dominant Negative (Odz-DN) activity. Embryos of the phenotypes: *odz*⁽³⁾⁸⁴⁴/*Df*(3)*odz*^{AL3} (a), and (b) *odz*⁽³⁾⁸⁴⁴/*Df*(3)*odz*^{AL3}; *P-HS-odzDN* demonstrates the dominant negative impact of the transgene Odz-DN. The heat shock-dependent cuticle phenotype was generated by raising embryos at 29°C, as in Experimental Procedures section. Cuticles were prepared as in experimental methods. Heads are oriented to the left.

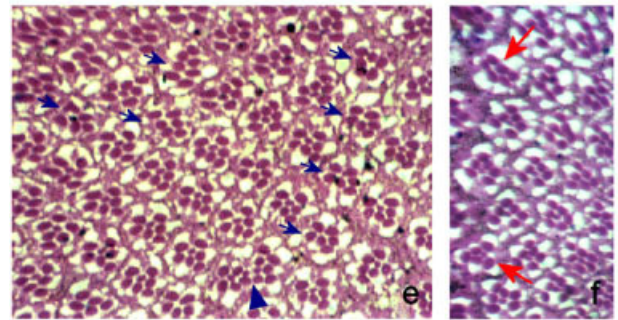
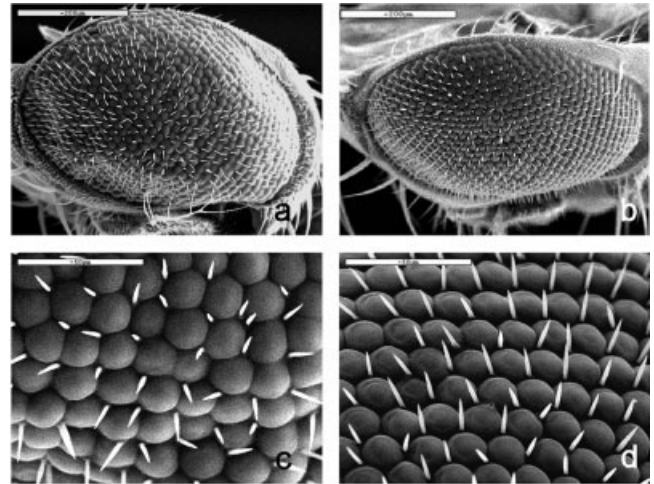


Fig. 3. Odz-Dominant Negative (Odz-DN) eye expression causes ommatidial disorder, misallocation of cells, and interommatidial bristle (IOB) defects. A UAS-Odz-DN transgene was driven by the GMR driver *w*; *P*{*w*[+*mC*]=*GAL4-ninaE.GMR*}12 at 29°C, with an accompanying control of the GMR driver alone cultured in parallel under identical conditions. **a,c,e–g:** GMR driver; **b,d,h:** GMR driver alone as controls for a, c, and g, respectively. **a,c:** Adult eyes in SEM with irregular ommatidial size, bristle defects, and fusions. **e,f:** Sections of adult eyes from GMR driven UAS-Odz-DN flies. Arrows indicate some of the ommatidia with an abnormal number of photoreceptor (PR) cells, or ommatidial fusions. **g,h:** Odz (brown) and Elav (black) immunocytochemistry. The staining is “compressed” where ommatidial founder spacing has lessened with Odz-DN expression (g) vs. without Odz-DN (h).

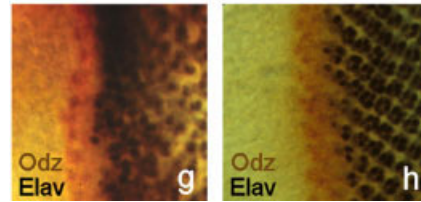


Fig. 3.

Fig. 4. *odz*- mitotic clones are very small relative to their twin spots. **a–d:** Adult eyes resulting from FRT-80B (chromosome 3L) “flips” to create mitotic clones marked by white gene dosage appear for *w-odz*- clones (c,d) and wild-type *w*- clones (a,b). Dark red patches represent twin spots carrying two *w*⁺ transgenes (see Experimental Procedures section). **a,b:** Control clones have identically sized twin spots. **c,d:** The *w-odz*- clones are very small relative to their associated neighboring twin spots.

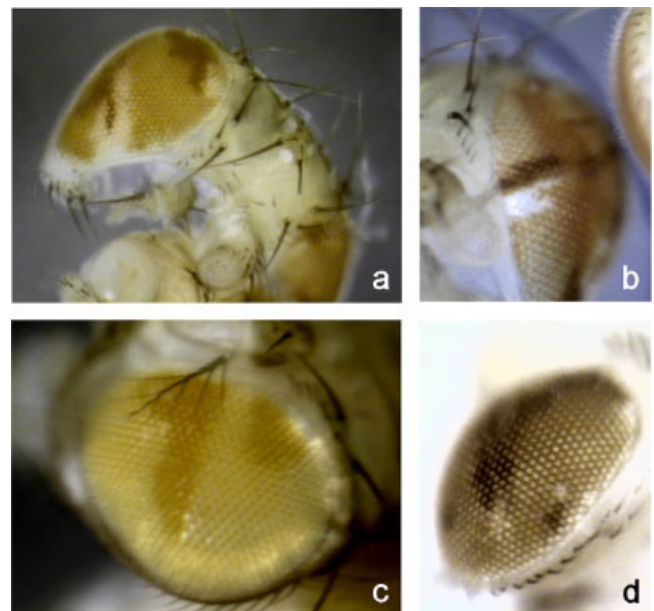


Fig. 4.

type I transmembrane protein (Levine et al., 1994; Dgany and Wides, 2002). It is, by many biochemical measures of the protein’s posttranslational modifications and membrane deployment,

analogous to the Notch protein (Dgany and Wides, 2002), despite its evident ability to dimerize (Feng et al., 2002). By modeling Odz transgenes on Notch dominant-negative transgene structures (Rebay et al., 1991), an Odz C-terminal truncation containing the first 1131 amino acids (aa) of the polypeptide (out of 2731 aa) was engineered. Protein expression from this transgene was proven under various induction regimens, including heat shock promoter-based leaky expression of the Odz carboxy-truncation protein in embryos raised at elevated temperatures (Dgany and Wides, 2002). The ability of the protein to function dominant negatively was proven through enhancement of the *odz* embryo cuticle phenotype. It enhances a weak allele combination of *odz*, which leads to very subtle segmentation defects (Fig. 2a; and Levine et al., 1997a), to a full fledged P-R phenotype (compare Fig. 2a and 2b), essentially phenocopying an *odz* null phenotype.

Odz-Dominant Negative Eye Expression Induces Distinct Eye Phenotypes

The Odz-Dominant Negative (Odz-DN) transgene caused similar phenotypic consequences under different induction regimens in the eye, including use of heat shock promoters or use of Gal4 lines to drive UAS-Odz-DN. Results only for the UAS-Odz-DN transgene driven by a single copy of GMR-Gal4 (Fig. 3) are, therefore, shown here. Flies carrying only GMR-Gal4 were cultured and examined simultaneously, with great care taken to establish conditions to minimize the phenotypic impacts of the GMR-Gal4-alone control (Fig. 3b,d; see Experimental Procedures section). Expression of the full-length Odz transgene induced no abnormal phenotypes (not shown). In contrast, expression of the Odz-DN transgene induced significant roughness in the adult eye (Fig. 3a,c). At high resolution, disruption of the spacing and order of ommatidial rows, loss of hexagonal shape for some ommatidia, and many scattered small and large ommatidia are observed (Fig. 3c). Partial and full fusions of

two or three ommatidia occur in the various regimens to varying degrees (see Fig. 3c). Many interommatidial bristles are missing, whereas supernumerary bristles, often close to regions of bristle loss, are seen (Fig. 3c).

Defects seen in sections of these adult retina are consistent with mis-spaced ommatidia and loss of specific cell types. First, several ommatidia have only six, and sometimes five, PR cells (Fig. 3e,f). Judging by the cross-sectional size and shape of the PRs' rhabdomeres, the cells often absent are R7, while visible light PRs are missing in other ommatidia (Fig. 3f, arrows). There are also ommatidia with more than seven PR cells visible, and fusions between ommatidia. This finding includes complete fusions where 12 and more PRs can be seen with no support cells between them (Fig. 3e, arrowhead). Third instar larval eye discs with induced Odz-DN (Fig. 3g) show a "compression" of the earliest Odz-expressing ommatidial clusters. The clusters appear as only one to two rows of Odz staining before Elav expression.

Mutant *odz* Clones Are at a Proliferative Disadvantage to Wild-Type Tissue

To more conclusively view the impact of loss of *odz* activity on eye development, we embarked on creating the means to observe *odz* mitotic clones. Homologous recombination of existing *odz* mutations onto a flippable FRT chromosome is extremely difficult due to the proximity of *odz* (at 79E on 3L) to the only appropriate available centromere-proximal FRT insertion on the chromosome (at 80B; see Experimental Procedures section). This was rendered virtually impossible by the selectable marker's (Neo) activity loss in FRT-80B stock lines (note in Flybase, Bloomington). To create flippable *odz* mutant lines, we instead EMS mutagenized the existing FRT-80B chromosome (one proven to truly have only one FRT; see Flybase), then screened for loss of viability across from an *odz* lethal mutation (see Experimental Procedures section). The resulting allele isolated and used here, *odz*⁶²⁸, is a lethal mutation on

an FRT-80B chromosome. While lethal, it gives only a mild, partially penetrant cuticle segmentation defect phenotype. It was outcrossed to unlink any other third chromosome lethals. It fails to complement to viability any *odz* allele tested. It makes no apparent protein (data not shown), but according to its nonamorphic cuticle phenotype, is not a null mutation.

The first obvious consequence of *odz* loss was very small mitotic clone size. Rather than being of equal size to their *odz*⁺ twin spots, as expected, the white *odz* clones were consistently several fold smaller than the dark red *odz*⁺ homozygous twin spots (Fig. 4c,d). This finding is in contrast to control white twin spots generated using the parental FRT-80B chromosome (see Experimental Procedures section), which gave equal size white and deep red twin spots (Fig. 4a,b). Whether the growth disadvantage of *odz* clones is due to failure to proliferate, promotion of cell death, or differential differentiation and survival is not clear. What this did mean was that assessing other *odz* functions in the eye, in clones typically covering a very small number of ommatidia, was difficult (see below). Many clones were in fact missed altogether, when a white spot was not detectable to point to the less prominent dark red twin spot generated from the "flip."

To verify that this survival disadvantage was independent of an eye specific differentiation or proliferation function, we also looked at flipped *odz*⁶²⁸ mitotic clones in other tissues. In the wing, *odz*⁻ clones are marked with *mwh* (*multiple wing hairs*), and *odz*⁺ homozygous clones are marked with *f* (*forked*) wing trichomes due to lack of an *f*⁺ transgene in an *f*^{36a} background (see Experimental Procedures section; Resino et al., 2002; Fig. 5a). Schematic representation of the clone distribution in a typical sampling of wings demonstrates that the *odz* mutation also confers the same growth or survival disadvantage to wings (Fig. 5d-g). In contrast, in twin spots created by this method using the parental wild-type FRT chromosome, the twin clones were of identical size

(Fig. 5b,c). Thus, proliferative disadvantage is imparted even by a hypomorphic *odz* allele. It must also be noted that alternative alleles will be

necessary to fully rule out the possibility that the *odz*⁶²⁸ clone death might be due to a lethal at a second locus on 3L.

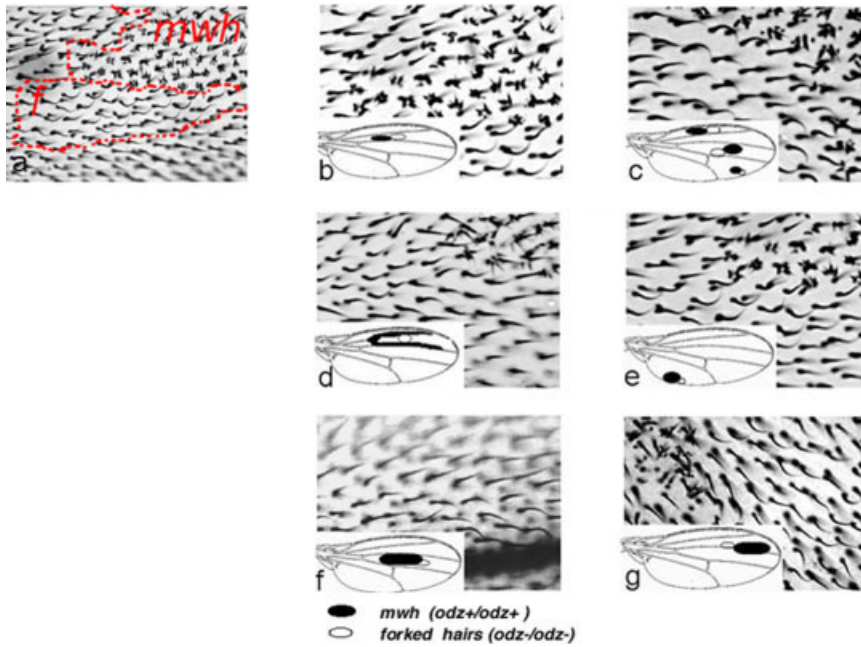


Fig. 5. *odz*- mitotic clones in the wing validate the necessity of *odz* for growth or survival. Twin spot wing clones were generated such that *odz*- clones are genetically marked with the mutation *multiple wing hairs* (*mwh*-), and their twin spots with *forked* (*f*-; see Experimental Procedures section). **a:** Adjacent clones marked with *mwh*- and *f*-. **b,c:** Controls with *odz*+ *mwh*- clonal patches. **d-g:** Experiment with *odz*- *mwh*- clonal patches. The area of the twin spots are schematically displayed for the entirety of the wing for the examples, with the *mwh*- region marked as white, and the *f*- sector marked as black.

Mutant *odz* Clones, and *odz* Clones in a Minute Background Show the Roughness, Ommatidial Fusions, and PR and Sensory Bristle Defects Seen in *Odz*-DN Eyes

A closer look at the largest of white *odz*⁻ clones shows a variety of defects (Supplementary Figure S1, which can be viewed at <http://www.interscience.wiley.com/jpages/1058-8388/suppmat>). However, a more extensive examination was attainable in *odz*⁻ clones generated in a Minute (*M*) background (Figs. 6, 7). Both regimens yielded the same results and mutant phenotypes, so those of the Minute clones are primarily addressed here. Crosses were designed to create *odz*⁻ clones lacking *M(3)*ⁱ⁵⁵ within a heterozygous background with one copy of Minute, and adjacent to a twin spot with two copies of *M(3)*ⁱ⁵⁵. This proffered the *odz*⁻ clone a significant growth advantage, despite its proliferation defect, and proved that the mutant's growth retardation capacity was not without limit (Fig. 6a). However, if a future

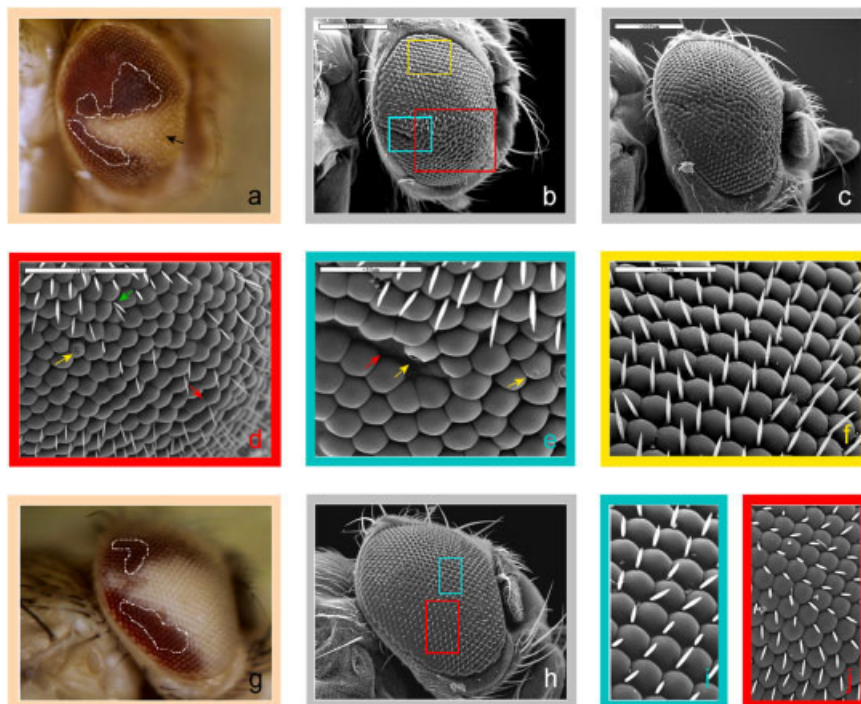


Fig. 6.

Fig. 6. *odz*- clones observed in a Minute background reiterate *Odz*-Dominant Negative (*Odz*-DN) defects. Adult eyes were mounted on scanning electron microscopy (SEM) discs, and were photographed in color before gold deposition and SEM. In this way, a comparison between the color and SEM photomicrographs allowed for genotyping of different portions of the mosaic eye as they appear in SEM. **a-f:** *odz*- *w*- clones in a Minute *M(3)*ⁱ⁵⁵ background (see Experimental Procedures section) are of significant size, due to their lack of the Minute mutation. They show abnormal ommatidial shape, size and order; interommatidial bristle (IOB) (interommatidial bristle) loss, and supernumerary IOBs at clonal margins. Note that a and b show the same eye in exactly the same orientation; c shows the eye at a slightly different angle to emphasize defects; and that d, e, and f are color coded enlargements taken from b. **g-j:** Wild-type *w*- control clones are very large in the Minute background, and show no defects. Again, g and h show the same eye in exactly the same orientation, and i and j are color coded enlargements taken from h. Black arrow, *w*- *odz*- clones; white dotted lines surround *w*+/*w*+ clones; red arrow, ommatidial fusion or region lacking ommatidia; green arrow, supernumerary IOBs; and yellow arrow, lens "breach."

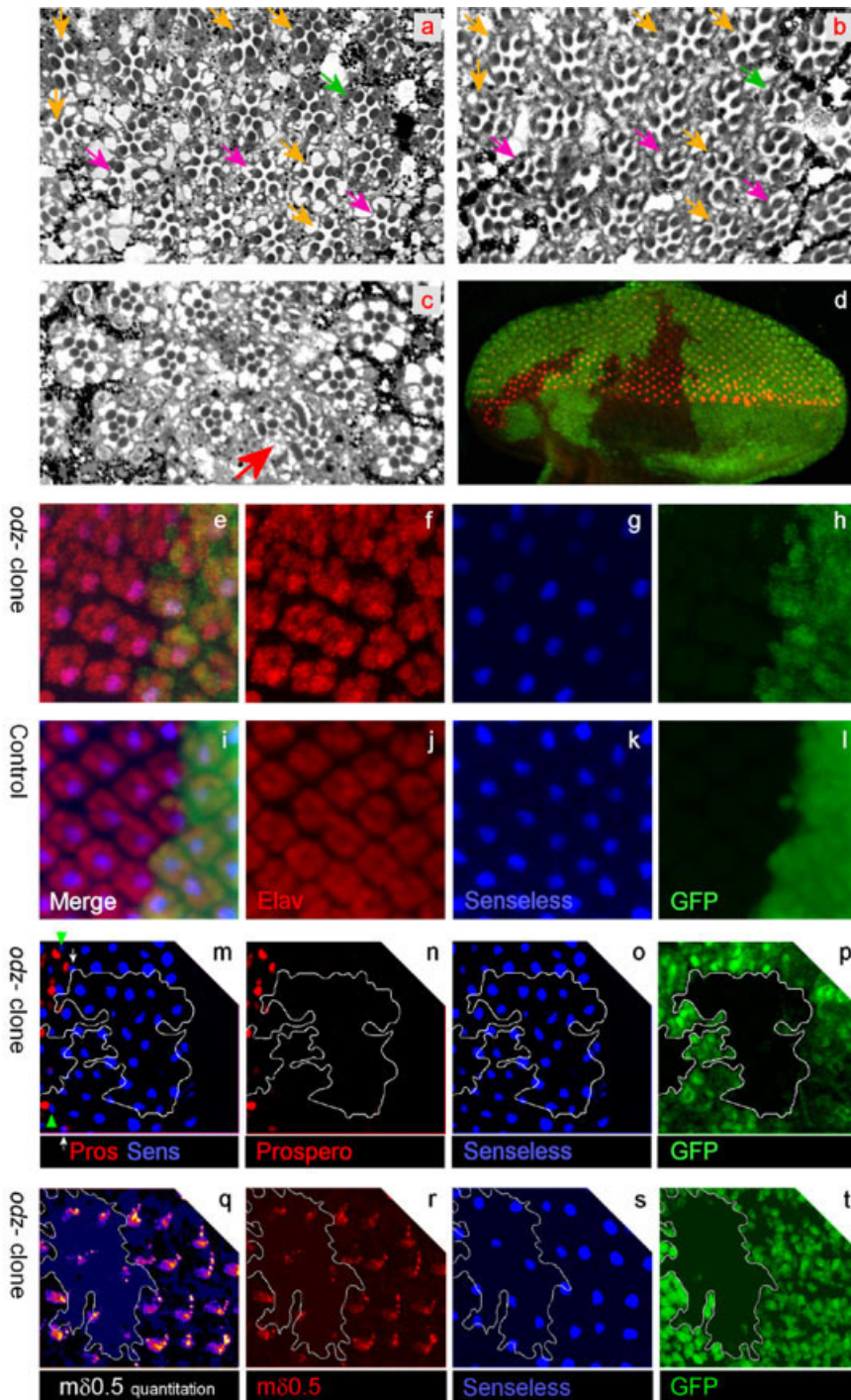


Fig. 7.

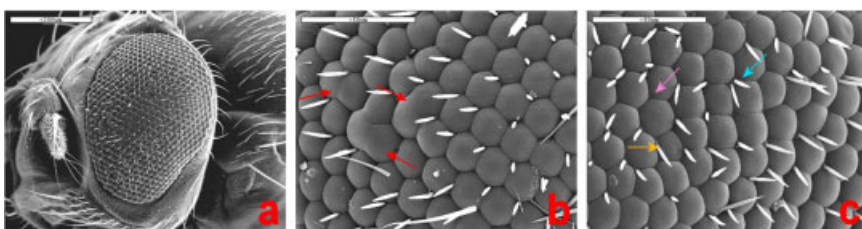


Fig. 8.

odz null displays no proliferation, an absolute requirement for growth will be assumed. In any case, the *odz* clones reached significant sizes, and could be better examined for pattern and specification phenotypes.

Eyes with clones were photographed in color after mounting the flies during preparation for scanning electron microscopy (SEM; see Experimental Procedures section). These samples then had their preparation completed and were subjected to SEM, with attention given to replicate the same image and angle of the eye (e.g., see Fig. 6a,b). The SEM results can

Fig. 7. *odz*-clones observed in a Minute background lose specific cell types and display subtle ommatidial spacing defects, disorder, and photoreceptor (PR) loss and alteration. **a-c:** Sections of adult eyes from *odz*-clones in the *M(3)⁵⁵* background. Note that all tissue except for the *odz*-clones show granular *w⁺* pigment at the periphery of the ommatidia. **a,b:** From serial sections of exactly the same region of a clone at the level of R7 cells (a) and R8 cells (b). Ommatidia lacking an R7 cell are marked with an orange arrow at both sectioned levels (a and b). Those lacking one or more visible light photoreceptors are marked with a pink arrow or a green arrow, respectively. **c:** The red arrow marks an ommatidial fusion. **d:** Senseless expression (red) in an *odz* clone. The clone region is distinguishable by lack of green fluorescent protein (GFP) staining (green). **e-h:** Senseless (blue) and Elav (red) in *odz*-clones are distinguishable by the lack of GFP (green). **e:** The merged probes in these *odz*-clones in a Minute background. **i-l:** Control clone with no loss of Odz activity in a Minute background. **m-p:** Prospero expression in an *odz* clone (anterior right, posterior left). **m:** White arrows flank the column of R8 cells (Senseless, blue) in ommatidia that express Prospero (red) only in R7. Green arrowheads flank the column of R8 cells in ommatidia that express Prospero strongly in R7, and begin to express it weakly in cone cells. Loss of Prospero in prospective R7 positions is observed. **n-p:** Prospero expression in an *odz* clone (anterior right, posterior left). **m:** White arrows flank the column of R8 cells (Senseless, blue) in ommatidia that express Prospero (red) only in R7. Green arrowheads flank the column of R8 cells in ommatidia that express Prospero strongly in R7, and begin to express it weakly in cone cells. Loss of Prospero in prospective R7 positions is observed. **q-t:** *mδ0.5-lacZ* N activation E(spl) reporter that marks R4 cells. **r:** Expression level of *mδ0.5* (red) is reduced in R4 cells within the *odz* clone. **q:** Another view of *mδ0.5* levels in the same R4s displayed with color-coded pixels representing increasing *mδ0.5* intensity values from black (weakest) to blue, pink, red, orange, then yellow (strongest).

Fig. 8. UAS-Odz-Dominant Negative (DN) driven by a Sca driver induces the same phenotypes as other Odz knockdown regimens. **a-c:** UAS-Odz-DN driven by a Sca-Gal4 driver induces all of the phenotypes seen in *odz*-clones or when Odz-DN is driven in the entire eye by GMR. Interommatidial bristle (IOB) loss, supernumerary IOBs, uneven ommatidial size and shape, column disorder, and ommatidial fusions are observed.

then directly be cross referenced to clone positions in these eyes (Fig. 6a–f). Ommatidial disorder is very striking in the *odz* clones (Fig. 6b,c,e). In contrast, as soon as the clonal border is crossed into surrounding areas, order is unperturbed (top of Fig. 6c,e, and all of 6f). Gross irregularity of ommatidial size occurs in *odz*⁻ tissue, together with loss of any semblance of hexagonal shape (Fig. 6d). Entire ommatidia appear missing within the *odz* clones (Fig. 6e), ommatidial fusions occur (Fig. 6d), and the lens of some ommatidia have a “hole” or “breach,” likely due to absent or malfunctioning lens-making cone cells (Fig. 6c,e; Frankfort et al., 2004). The loss of sensory bristles is complete within the clones, while the interommatidial bristles (IOBs) are fully present in surrounding heterozygous and twin spot areas (top of Fig. 6c,e, and all of 6f). Supernumerary bristles can be seen at the border of the clones (Fig. 6c). Thus all of the defects seen due to *Odz*-DN expression are recapitulated here. None of these defects are seen in control clones (Fig. 6g–j).

The sectioned adult eye reiterates the suite of specific defects documented for *odz*-DN eyes (Fig. 3e,f). One region of a large clone is displayed sectioned at the level of R7 cells as well as at the level of R8 cells (Fig. 7a and 7b, respectively; from serial sections). The *odz*⁻ clone sections have several ommatidia with only six, and sometimes fewer, PR cells appearing at the R7 level (Fig. 7a,c). Judging by the morphology and a comparison between the R7 and R8 level sections, R7 PR cells are often those absent (Fig. 7a,c). Also common is loss (seen at both the R7 and R8 level) of a single visible light photoreceptor, often R6, based on position (Fig. 7a–c). There are a much smaller number of ommatidia with more than one missing PR (Fig. 7a,b). No R8 loss occurs. There are also ommatidia with more than seven PR cells visible, indicating fusions between ommatidia (Fig. 7c). Most frequently, the loss of proper orientation of the ommatidia, likely due to improper rotation, can be discerned when comparing to the orientation of the pigmented wild-type ommatidia that surround the clones (Fig. 7a–c). More than one-third of the ommatidia within clones in a

Minute background are rotationally disoriented, and one-quarter to one-third of the ommatidia within clones in a Minute background are missing at least one photoreceptor. Among the ommatidia with an abnormal PR count, approximately half have no R7 cell, half are missing a visible photoreceptor, less than five percent have lost more than one photoreceptor, and less than five percent are ommatidial fusions.

***odz* Acts Downstream of R8 Specification, With Impacts on Specific Cell Types**

odz clones in a Minute background were examined at the larval stage for expression of Senseless protein. Expression of *senseless* (*sens*) within emerging intermediate groups, in R8 equivalence groups, then in individual R8 cells, indicates the commitment to R8 sensory neuronal fate differentiation of a cell emerging from the post-MF proneuronal cluster (Frankfort et al., 2001). Senseless is expressed in the *odz* clone, in a distribution once per ommatidial unit (Fig. 7d). Thus *Odz* is not required for the specification of the pro-neuronal units or R8 identity. Cells subsequently recruited around each R8 display disrupted placement and uniformity of order, as emphasized by *Elav* staining (compare Fig. 7e–h to 7i–l). Assessment of markers for the fate of given types among these cells was undertaken in *odz* clones.

Prospero functions in Sevenless-competent cells before Sevenless signaling, and encodes a transcription factor that responds to RAS1 through RTK signaling. Its expression appears initially in developing R7 cells, then subsequently in cone cells, while R7 expression increases to exceed that emerging in the cone cells (Kaufmann et al., 1996; Fig. 7m–p). By observing the two most anterior Prospero expressing columns of cells crossing an *odz* clone, we distinguish positions lacking expected R7 precursors (see Fig. 7m). Not all, but a large majority, of expected R7 precursors are missing from *odz* clones according to Prospero staining. This finding is consistent with the loss seen for R7 cells in adults (see Fig. 7a).

The transgene *mδ0.5* reports on a

subset of the enhancers that drive *E(spl)* expression, and is specific for R4 (Cooper and Bray, 1999). Within *odz* clones, the expression of *mδ0.5* in the R4 precursors is reduced (30% of the level of wild-type, see Experimental Procedures section; and Fig. 7q–t). Attenuated R4-specific expression of *E(spl)* attests to lowered N signaling and possible subsequent visible photoreceptor fate alteration. This could potentially be expressed as altered specification or fates of R4 cells themselves, or of cells with which R4 interacts. An assessment of these, and of other cell types' development will be studied with further markers in the future.

Scabrous-Driven *Odz*-DN Transgenes Replicate *odz*⁻ Phenotypes

Scabrous (*Sca*) modulates the initial step of proneuronal clusters' commitment to neuronal fate and atonal expression at the furrow. It is then key, through its interaction with Notch, for lateral inhibition between the preclusters to establish proper ommatidial founder spacing (Baker and Zitron, 1995; Ellis et al., 1994). *Sca* expression occurs before and in the intermediate proneuronal groups, R8 equivalence groups, and subsequent four columns of R8 precursor cells (columns 0–3). We “drove” *Odz*-DN expression using a *Sca*-Gal4 transgene driver, to locally knock down *odz* activity at and immediately after the furrow. Given the cell membrane association of *Odz*, we would expect the *Odz*-DN construct to have an effect on endogenous *Odz* only if the transgene and endogenous gene are expressed in cells at most one cell away. In fact a strong series of phenotypes are seen from *Odz*-DN driven in *sca*-expressing cells (Fig. 8a–c), but not with the control UAS-*odz*-DN transgene without the driver (not shown). Disruption of order, fusion of ommatidia, great variance of ommatidial size, missing IOBs, and occasional supernumerary bristles are observed. Thus the collection of phenotypes replicated again here must be caused by the inactivation of *Odz* at or posterior to the furrow, and not due to later expression of *Odz* (e.g., see arrowhead in Fig. 1a; and below).

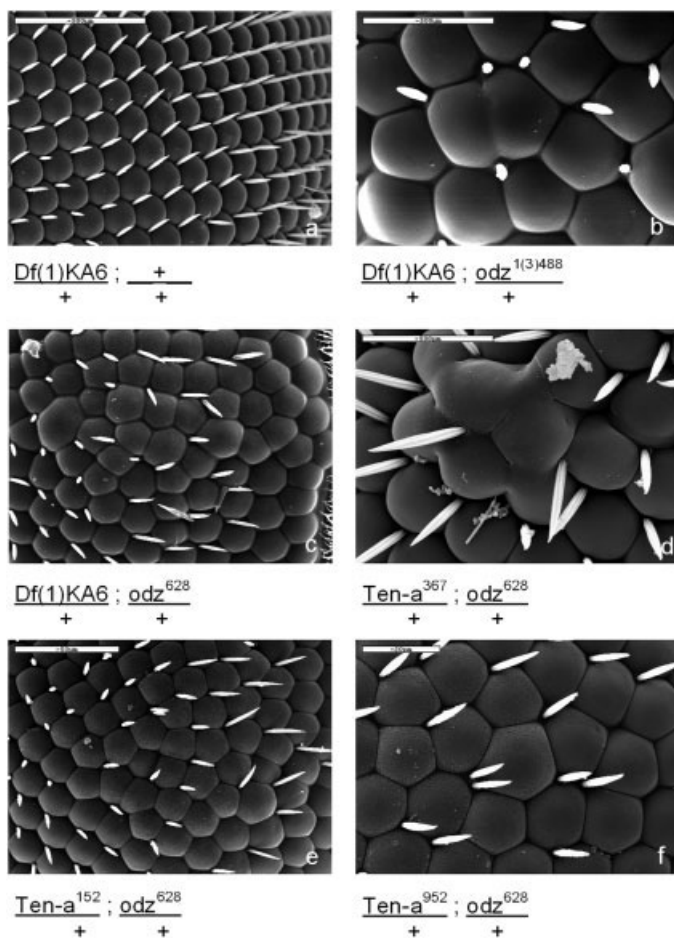


Fig. 9. *Ten-a* and *odz* transheterozygous combinations phenocopy *Odz* knockdown regimens. **b–f:** Transheterozygous *Ten-a* (deficiency or single mutation) *odz* combinations give all of the phenotypes associated with *Odz* loss-of-function regimens above. Interommatidial bristle (IOB) loss, supernumerary IOBs, uneven ommatidial size and shape, column disorder, and ommatidial fusions are observed. **a:** *Ten-a* deficiencies (and single mutations, not shown) do not give these phenotypes when alone.

odz and Its Paralog *Ten-a* Synergize to Recapitulate the Same Eye Defects

The *Drosophila Ten-a* gene is paralogous to *odz* (Fascetti and Baumgartner; 2002), and directs patterning in several tissue contexts (Rakovitsky et al., manuscript submitted for publication). Embryos from germ line clone-derived eggs lacking both maternal and zygotic *Ten-a* contribution display an *odz* like P-R phenotype (Rakovitsky et al., manuscript submitted for publication). Nonlethal lesions exist among *Ten-a* alleles, some of which homozygously give rise to rough eyes at very low frequencies (Rakovitsky et al., manuscript submitted for publication). No *Ten-a* allele shows eye phenotypes as a heterozygote (Fig. 9a). Nonetheless, eye phenotypes result-

ing from *odz/Ten-a* transheterozygous allele combinations appear at significant frequencies (see examples in Fig. 9b–f). These range from 21% to 40% of adults with clear phenotypes when using a *Ten-a* covering Deficiency (40%), or lethal point mutations (21–30%; Fig. 9b–d), or 5–6% with other *Ten-a* lethal point mutations (Fig. 9e,f). All of the phenotypes caused by *odz* loss of function genotypes, which we have described above, are seen here to exaggerated extents due to synergy of partial *odz* and *Ten-a* loss. Irregular ommatidial size, loss of hexagonal ommatidial shape, two and three unit ommatidial fusions, bristle loss, disordered placement of sporadic supernumerary bristles, and widespread disorder and spacing defects are reiterated in these strong phenotypic

examples (Fig. 9b–f). These transheterozygous effects strongly suggest that *Odz* and *Ten-a* closely, if not directly, cooperate. The striking synergy is consistent with data suggesting that *Odz* and *Ten-a* can form heterodimers (unpublished observations), as has been established for all four vertebrate homologs (Feng et al., 2002). We think it likely that *Ten-a*, whose expression overlaps that of *Odz* (unpublished observations), acts together with *Odz* to exert its functional effects in the eye at the stages that we have documented for *Odz* alone.

DISCUSSION

Odz Is Necessary for Several Cell Types of the *Drosophila* Eye

While unable to examine the effect of complete loss of activity of the P-R gene *odz* in *Drosophila* eyes, we carried out several varied *odz* loss of activity regimens, all of which produced the same constellation of eye phenotypes. The approaches included use of an *Odz*-DN protein expressed broadly in the eye (with *GMR*) or in *Sca*-expressing cells in and posterior to the furrow; producing eye clones with an *odz* hypomorphic allele in a normal or *Minute* background; and producing *odz/Ten-a* transheterozygous allele combination flies. The consistently produced phenotypes were changes in ommatidial shape, order, orientation, and size; ommatidial fusions; IOB loss; and lens “breaches” likely due to cone cell defects. Eyes that were sectioned revealed variable photoreceptor loss: visible; and especially of R7. The consistency of the phenotypes from these very different “knock-downs” supports their validity, despite the lack of a null *odz* experiment. The phenotypes will perhaps be more penetrant and robust in an *odz* null, but it remains to be seen if distinct additional phenotypes will arise with a null.

Odz is expressed in cells of ommatidial preclusters in columns 0–3, immediately posterior to R8 equivalence groups. *Odz* is expressed after the earliest *Senseless* expression (Fig. 1d,g), and after R8 specification, as evidenced by the presence of *Senseless* expression in *odz* clones (Fig. 7d). No

adult ommatidia were observed that lack an R8 photoreceptor in *odz* knockdowns (Fig. 7b), further attesting that *odz* does not participate in R8 specification. Instead, high transient *Odz* expression occurs in emerging photoreceptors in and posterior to the furrow in prospective R8, 2, 5, 3, and 4 cells, according to cluster placement and morphologies (Fig. 1k). This *Odz* expression is at a stage and position appropriate to possibly impact: early ommatidial positioning, such as spacing and rotation; decisions taken during the above-mentioned five cells' differentiation; specification of the above four visible PR precursors; and fates of later recruited cells that these five cells contact or less directly influence. Observed *Odz* loss leads to loss of cell order within ommatidia, rotation defects, but only inconsistently to ommatidial spacing defects. Among these cells, we documented marker changes in only one precursor, R4, with *odz* loss causing down-regulation of the *m80.5* reporter of *E(spl)* expression and *N* activation. Although this R4-specific signaling change is significant, we must still clarify ultimate R4 fate, and must examine the fate of the other PRs.

At a later stage, the loss of primarily R7 photoreceptors seen in adult *Odz* knockdown ommatidia may result from two distinct possible causes. The first might be due to early order and spacing defects (above) subsequently causing local pools of precursor cells between forming ommatidial centers to be underpopulated or disorganized to the point that the last formed PRs (such as R7) fail to be recruited. This can also explain why subsequently recruited accessory cell types are also observed as lost in *Odz* knockdown tissue, and why sporadic ommatidial fusions are observed. The depletion of pools of precursor cells available for differentiation might also be influenced by *odz*⁻-induced cell death or faulty proliferation, in later larval and postlarval stages (see below). Alternatively, *odz*⁻ compromised fates of the five first PR precursors might interact with and change the specification of subsequently recruited cells.

The second distinct cause for the variety of specific cell type losses may be due to the need for *Odz* activity re-

peatedly in a series of distinct cell-type specific specification programs. It is possible that later larval *Odz* expression (Fig. 1l, 1a, arrowhead) is required for full development of R7 and other late cell fates. The fates of the visible PR cell types might also be dependent on the very low level of *Odz* expressed between the two strong expression fields, noticeable at high sensitivity (Fig. 1f,l). A more extensive identification of cells lost in eye disc clones must be carried out to complement the first view of the fates of R7 precursors, and of R4 precursor expression alterations.

Much later, *Odz* is also expressed subsequently in the pupal eye disc (data not shown), which may play a role in IOB and cone cell fates. Senseless expression occurs in pupal eye discs. IOB defects and evident cone cell defects leading to lens "breaches" observed for *Odz* are like those that occur with *senseless* loss (Frankfort et al., 2004). It is possible that *odz* cooperates with *senseless* in these contexts where their expression overlaps and where they yield similar mutant phenotypes.

Odz Mutants Cause Cells and Clones Not to Thrive

odz clones in the eye and wing failed to thrive. Further insight into the underlying molecular mechanism, or partners of *Odz*, was not derived here. However, that the smaller clone size is seen in adults, yet not in the original larval discs, means that it is a failure that occurs after the first steps of differentiation impacted by *Odz*, in late larval or pupal stages, through later, distinct processes. Whether the processes include differential survival, programmed cell death, or altered proliferation rates will only be answered with further work, as will an assurance that the failure to thrive is attributable solely to *odz*, and not to a second site mutation on the *odz*-FRT chromosome. However, we have seen that *Ten-a* clones are also smaller than their twin spots in eyes (Swissa and Wides, unpublished), suggesting that this is a bona fide phenomenon involving both paralogs, perhaps in concert.

Proposed Mechanisms of Odz-DN Activity

The rationale for constructing an *Odz*-DN transgene to encode a carboxy-terminal truncated form was to mimic known DN constructs of Notch (Rebay et al., 1991). The intracellular portion of Notch is necessary to propagate a signal sensed extracellularly by its N-terminal EGF region (see Artavanis-Tsakonas et al., 1999). Overexpression of a C-truncation, which can compete for ligand binding but which cannot provide a cleaved functional N^{ICD}, prevents intracellular transduction of the signal. Our extensive work on the *Odz* protein is summarized in our model of the protein as a type I transmembrane protein that is deployed to the plasma membrane as a linked pair of the N terminus (including EGF-repeats) covalently joined to a postcleavage C-terminal portion by a reducible bond (Dgany and Wides, 2002). *Odz* proteins of this structure undergo additional cleavages, intracellularly, and we assume that overexpressing a variant with an incomplete C-terminus disrupts a function needed intracellularly for *Odz*. In that sense, we propose that *Odz* acts, at least in part, by a Notch-receptor-like manner, involving cleavage. In addition, and unlike Notch, pairs of *Odz* N-terminal to C-terminal complexes associate as dimers (Dgany and Wides, 2002). Therefore, the formation of nonfunctional dimers is an alternative and perhaps complementary hypothesis for the basis of the dominant negative activity of the *Odz* C-terminal truncation.

Unlike our model, type II models for *Odz*/*Tenm* proteins have also been proposed by other groups (Oohashi et al., 1999; Rubin et al., 1999). They model a short N terminal portion of the protein as intracellular, followed by a highly hydrophobic region considered a transmembrane domain (as opposed to a signal peptide region by our analysis) and a large, C-terminal extracellular, globular portion (Oohashi et al., 1999). According to this model, it is possible to expect a failure of necessary dimerization mediated by extracellular domains (Feng et al., 2002) in the large C-terminal truncation we carried out. In fact, the carboxy-terminal truncation manipulation proved experimentally to confer dominant-

negative activity to Odz, and both models can conform to this result.

odz in Other Sensory Tissues

Odz expression and developmental and functional roles in sensory bristles are not limited to the IOBs (Levine et al., 1997b). Sensory bristles in the wing disc, sensitive to Ac/Sc, express *odz* during larval stages. Odz is also expressed in developing bristles in the leg disc and others, as well as developing chordotons and is imaged by *odz* enhancer trap lines even at adult stages in chordotons and external sensory organs (Levine et al., 1997b). There is also expression in the maxillary palp and antennae in the olfactory organs of *Drosophila*, just as there is in every olfactory epithelium of vertebrates examined (e.g., Otaki and Firestein, 1999; Ben-Zur et al., 2000). In fact, the peripheral nervous system, sensory ganglia in the central nervous system, and sensory tissues all have some Odz gene expressed in all vertebrates examined. The extent that here, too, Odz might contribute to sensory cell differentiation together with coexpressed Senseless in different contexts, remains to be determined.

Odz in the Eye Is Universal in Metazoans

Odz is expressed in the eye of all vertebrates examined. There are four paralog types, Odz/Ten1-4, in all vertebrates. Each of them has expression in some portion of the eye and visual system, as documented in rat, mouse, chicken, and zebrafish. This includes pigmented retina, neural retina, optic stalk, and expression in several important embryonic developmental sites of the eye (Oohashi et al., 1999; Minet et al., 1999; Rubin et al., 1999, 2002; Mieda et al., 1999; Otaki and Firestein, 1999; Tucker et al., 2001; Ben-Zur et al., 2000; Zhou et al., 2003). Perhaps most importantly, the first non-*Drosophila* Odz mutant, Odz4, yields developmental eye defects in the mouse embryo (Lossie et al., 2005). Given the nature of Odz and Ten-a function in the fly eye, and given the parallels found for many key patterning genes in the eye of *Dro-*

sophila proving to be critical for vertebrates, we expect that the roles in flies and vertebrates have a common evolutionary ancestry. It should prove to be an important patterning and differentiation gene to follow in vertebrates, within the developing frameworks of molecular control of eye development and differentiation.

EXPERIMENTAL PROCEDURES

Drosophila melanogaster

Stocks

D. melanogaster stocks were maintained at 25°C on standard corn meal–yeast–agar medium. *odz*⁶²⁸ is an EMS-induced hypomorph on an FRT third chromosome whose derivation is described below, whereas *odz*¹⁽³⁾⁸⁴⁴, *odz*¹⁽³⁾⁵³⁰⁹, and Df(3L)*odz*^{AL3} are as previously described (Levine et al., 1994, 1997a). Stocks carrying a transgene encoding a carboxy-terminal truncation of the Odz protein (Odz-DN), or a transgene encoding the full-length Odz protein, downstream of a heat shock promoter or a UAS promoter were prepared and are described as previously (Dgany and Wides, 2002), and below.

The GMR Gal4 driver *w*; P{w[+mC]=GAL4-ninaE.GMR}12 was obtained from the Bloomington *Drosophila* stock center. Sca-Gal4 (*w*; P{w+sca-Gal4}/CyO) and *sca*¹ were kindly provided by Adi Salzberg. The X chromosome deficiency Df(1)KA6/FM7c, which deletes 10E1-11A7-8 and which was proven to delete *Ten-a* (Rakovitsky et al., manuscript submitted for publication), was obtained from Bloomington. *Ten-a* mutants generated from inexact excisions of a resident nonlethal P-element insertion: *Ten-a*³⁶⁷/FM6B; *Ten-a*¹⁵²/FM6B; and *Ten-a*⁹⁵²/FM6B were generated and balanced as described (Rakovitsky et al., manuscript submitted for publication). Also obtained from Bloomington were Samarkand, Canton-S, and *y w*.

The 80B FRT carrying line *y*¹ *w*¹¹¹⁸; P{ry[+t7.2]neoFRT}80B (Chou and Perrimon, 1996) is described below, including deviations from its original description. The following lines were used for flipping the left arm of the

third chromosome: *y w* Hs-FLP 22; ubi-GFP, *M(3)**i*⁵⁵ P{ry[+t7.2]neoFRT}80B/TM6B, a line from the Antonio Garcia-Bellido lab kindly provided by Bertrand Mollereau; *w*; P{w[+mC]=Ubi-GFP.D}61EF P{ry[+t7.2] FRT}80B, obtained from Bloomington; and *y w* Hs-FLP 22; TM3 Sb/TM6B, obtained from Bloomington. Crosses between *w*; P{w[+mC]=Ubi-GFP.D}61EF P{ry[+t7.2] FRT}80B and *y w* Hs-FLP 22; TM3 Sb/TM6B yielded *y w* Hs-FLP 22; P{w[+mC]=Ubi-GFP.D}61EF P{ry[+t7.2] FRT}80B. A line used for creating marked mitotic clones in the wing, Hs-flp-9F *w*^{β6a}; *mwh* P{f⁺}64C P{FRT}80B/TM1, was a kind gift of the Antonio Garcia-Bellido lab. m80.5 (P{E(spl)m80.5-lacZ}(line 6F5, on chromosome II) is the enhancer of split isolated enhancer reporter that marks R4 specific Notch activation (Cooper and Bray, 1999).

Mutagenesis and Screening: Creation of an FRT-*odz* Mutant Chromosome

The FRT line bearing a single FRT element at 80B (*y*¹ *w*¹¹¹⁸; P{ry[+t7.2]neoFRT}80B), but lacking encoded Neo function as reported (www.flybase.org), was obtained from Bloomington. Despite reports of an unexpected second FRT P element on 80B FRT lines, this stock was verified to have only one P element at 80B. Homozygous males of this line were ethyl methane sulfonate (EMS) mutagenized by overnight feeding of 25 mM EMS in a 1% sucrose solution. Twenty-four hours after feeding, those males were crossed to *y w*; *Xa*/TM3 *Sb* females, and all Stubble marked male offspring were collected. Three thousand such males were pair crossed to *y w*; *odz*¹⁽³⁾⁵³⁰⁹/TM3 *Sb* females, and crosses that produced only Stubble offspring were saved. Five such families were kept as lines, and each represented a mixture of flies carrying *odz*¹⁽³⁾⁵³⁰⁹ over the balancer plus a mutation that failed to complement *odz*¹⁽³⁾⁵³⁰⁹ over the balancer. Six to ten male offspring from each of these lines were backcrossed to *y w*; *Xa*/TM3 *Sb* females in pair crosses, and the six to ten resulting sublines were evaluated to see whether the subline founder parent

bore *odz*^{l(3)5309} or the new *odz* allele on the FRT chromosome.

The two options were differentiated by their ability to support a polymerase chain reaction (PCR) using the primer pair *acaagcaaacgtgcactg* and *tgtattgacggtgtgtttgtttg*. The primers support a PCR product of 250 bp between a point within the disrupting P element of *odz*^{l(3)5309} and the flanking downstream genomic *odz* DNA at 79E. The newly mutagenized chromosome, with a P element only at 80B bearing the FRT, produces no PCR replicon with this primer pair. The sublines, once isolated, were outcrossed to unlink other third chromosome lethals, then were tested and proven not to complement other known *odz* alleles and deficiencies. The *odz*⁶²⁸ (*w*⁻; *odz*⁶²⁸ FRT80B)/TM3 Sb line used in this work bears a mutation on the FRT chromosome that is lethal but that has a very weak P-R cuticle phenotype, like many other lethal *odz* hypomorphic alleles (Levine et al., 1997a). Line *odz*⁶²⁸ was balanced with a TM3 Sb *ftz-LacZ* chromosome, allowing for selection of homozygous *odz* embryos that are not stained blue in the presence of X-Gal. A handpicked population of the *odz*⁶²⁸ homozygous embryos yields protein extracts with no Western detectable Odz protein, unlike sibs carrying one or two wild-type *odz* alleles (for Experimental Procedures section, see Dgany and Wides, 2002).

Genetically Marked *odz*⁻ Wing Clones

Clones of *odz* and accompanying twin spots in the wing were marked by a *forked* (*f*) and *multiple wing hairs* (*mwh*) FRT technique (see Resino et al., 2002). Female Hs-*flp-9F w*^{β6a}; *mwh* P{f⁺}64C P{FRT}80B /TM1 flies were crossed to *odz*⁶²⁸ P{ry[+t7.2]neoFRT}80B/TM3 Sb males, and offspring were heat shocked at early larval stages. The resulting males not carrying balancers were capable of yielding *forked* marked *odz* clones and their associated *mwh* marked twin spots upon "flipping." For non-*odz*⁻ controls, female *hs-flp-9F w*^{β6a}; *mwh* P{f⁺}64C P{ry[+t7.2] neoFRT}80B/TM1 flies were crossed to P{ry[+t7.2]neoFRT}80B males, followed by the same treatment. The areas of the twin spots were photographed

and examined. Schematics of the relative twin spot clone sizes were drawn accordingly.

Genetically Marked *odz*⁻ Eye Clones

y w; *odz*⁶²⁸ FRT80B/TM3 Sb males were crossed to *y w* Hs-FLP 22; P{w[+mC]=Ubi-GFP.D}61EF P{ry[+t7.2] FRT}80B females. Offspring were heat shocked as first instar larvae, and all non-Stubble flies were capable of "flipping" that yields white, non-green fluorescent protein (GFP) carrying *odz*⁻ clones adjacent to deep red twin spots encoding enhanced GFP expression. At late larval stages, eye discs were examined by confocal microscopy for clonal twin spots marked by GFP autofluorescence. Half of all eye discs, those with two 80B-FRT bearing chromosomes, are capable of developing mitotic twin clones. As adults, clonal twin spots were identified according to White pigment, potentially in all non-Stubble flies.

To generate *odz*⁻ clones of enhanced size, *y w*; *odz*⁶²⁸ FRT80B/TM3 Sb males were crossed to *y w* Hs-FLP 22; *ubi-GFP*, *M(3)*ⁱ⁵⁵ P{FRT 80B}/TM6B females. One-quarter of both male and female offspring are capable of developing mitotic twin spot clones. As adults, those capable of producing mitotic clones are evident due to their lack of the balancer chromosomes' genetic markers, and those that actually bear clones are evident by white pigment. GFP expression, which was relatively weak, was imaged in discs using anti-GFP antibody. To generate *odz*⁻ clones for following R4 cells and Notch activation, *y w*; *odz*⁶²⁸ FRT80B/TM3 Sb females were crossed to *mδ0.5* males. Non-Sb, *odz*⁶²⁸-resulting F1 males were crossed to *y w* Hs-FLP 22; P{w[+mC]=Ubi-GFP.D}61EF P{ry[+t7.2] FRT}80B females. The F2 offspring were heat shocked as first instar larva. Half of the F2 offspring are capable of developing mitotic clones, among which half carry *mδ0.5-lacZ*. The relevant flies' genotype is *y w* Hs-FLP/*y w*; *mδ0.5-lacZ*/+; *odz*⁶²⁸ FRT80B / P{w[+mC]=Ubi-GFP.D}61EF P{ry[+t7.2] FRT}80B. Discs were examined with anti-GFP and anti-βGal antibodies.

DNA and Transgenics

A 3.6-kb *EcoRI* fragment of the Odz cDNA clone p9.1 (Levine et al., 1994) was ligated into the *EcoRI* site of the polycloning stretch of pCaSpeR-UAS or pCaSpeR-hs. These yielded transgenes that encode an 1131-aa carboxy-truncation of the Odz protein. These transgenes, and corresponding full-length Odz encoding transgenes, were injected into syncytial embryos to generate transgenic lines by modifications of standard methods.

Genetic Crosses

A line that was balanced for the *odz*^{l(3)844} mutation, and also carried two copies of HS-Odz-DN on the second chromosome was created. This line, and the original *odz*^{l(3)844} line, were crossed with Df(3L)*odz*^{AL3} to generate the weak allelic combination *odz*^{l(3)844}/Df(3L)*odz*^{AL3}, with and without the HS-Odz-DN transgene, respectively. The flies were raised at 29°C, and the "leakiness" of the HS promoter was adequate to induce effective Odz-DN levels to observe enhanced cuticle phenotypic effects. This observation was achieved with several different insertions of the transgene and was heat dependent. Cuticle phenotypes were examined after preparation of embryos by standard methods (Wieschaus and Nusslein-Volhard, 1986).

Balanced *odz* and *Ten-a* lethal lines were crossed, and offspring transheterozygous for the *Ten-a* and *odz* alleles, as evidenced by absence of balancer's markers, were examined. Ommatidial phenotypes, as visualized by SEM micrographs of compound eyes, were examined.

Crosses were carried out between appropriate lines to bring together Gal4 drivers and UAS transgenes, under conditions of 29°C for maximal expression, unless otherwise noted. GMR drivers were carefully controlled, as driver alone, in the same incubations and regimens as experiments, as were all other drivers, such as *Sea*, when used to drive Odz-DN and Odz-full-length.

SEM and Adult Eye Sections

Light microscopy of sectioned adult *Drosophila* eyes (Tomlinson and

Ready, 1987) and SEM of adult *Drosophila* eyes were prepared, examined, photographed and analyzed by modifications of standard methods. For SEM work, flies were mounted on the SEM sample preparation discs by standard procedures. The eyes of these flies were photographed in a binocular microscope at ideal angles to view the color of the red heterozygous tissue plus white and deep red twin clone spots. After gold coating, the eyes of the samples were examined and photographed in SEM. Great care was taken to photograph the SEM micrographs in precisely the same orientation and angle as the previously recorded color pictures. In this way, a clear correlation can be made between any portion of the eye and its twin-spot genotypes according to White pigment.

Antibodies and Immunocytochemistry

The anti-Odz mouse monoclonal antibody MAb20 has been described (Levine et al., 1994). Monoclonal rat (7E8A10) and mouse (9F8A9) anti-Elav antibodies were obtained from the Developmental Studies Hybridoma Bank (DSHB). Monoclonal mouse anti- β gal antibody (40-1a) and mouse anti-Prospero (MR1A) antibody were also obtained from DSHB. Guinea pig anti-Senseless antisera was a kind gift of the lab of Hugo Bellen. Rabbit anti-GFP antisera was obtained from Molecular Probes, Invitrogen (Eugene, OR; catalog number A11122). Secondary antibodies conjugated either to horseradish peroxidase (HRP; Jackson Laboratories, West Grove, PA) for diaminobenzamide (DAB) turnover or fluorescent molecules (below) were used. Nuclear staining was achieved by brief exposure to Hoechst stain.

Third instar larva were dissected and their eye-antennal discs were treated for immunocytochemistry as described (Levine et al., 1997b). HRP-based double immunocytochemical staining of Odz and Elav was performed as follows. Odz was visualized first using mouse anti-Odz followed by goat anti-mouse HRP and DAB development under standard conditions. The simultaneous rat anti-Elav reaction was then followed by goat anti-rat

HRP and DAB development in the presence of nickel chloride and cobalt chloride to yield a black reaction. For immunofluorescence confocal microscopy, the secondary antibody conjugates used were anti-mouse Cy3, anti-mouse Cy5, anti-guinea pig Cy2, anti-guinea pig Cy3, anti-guinea pig Cy5, anti-rabbit Cy2, and anti-rat tetramethylrhodamine isothiocyanate-rhodamine (all from Jackson Laboratories). The β gal staining driven by $m\delta 0.5$ in R4 cells was quantitated by integrating fluorescence intensities for an entire stack of Z-sections of the relevant eye clones, and surrounding tissue (control), to capture expression in the entire relevant "spatial volume."

ACKNOWLEDGMENTS

Many thanks to Nick Baker and Adi Salzberg for *sca*¹ and Sca-Gal4 Driver flies, Hugo Bellen for anti-Senseless antibody, Bertrand Mollereau for Minute bearing FRT lines, Antonio Garcia-Bellido for FRT - *f* lines, Judy Hanania for expert assistance, and Adi Salzberg for critically reading this manuscript. Thanks also to Assaf Amitai, Shirley Brenner, Vita Frager, and Nadya Rakovitsky for careful reading of the manuscript.

REFERENCES

Adams MD, Celniker SE, Holt RA, Evans CA, Gocayne JD, Amanatides PG, Scherer SE, Li PW, Hoskins RA, Galle RF, George RA, Lewis SE, Richards S, Ashburner M, Henderson SN, Sutton GG, Wortman JR, Yandell MD, Zhang Q, Chen LX, Brandon RC, Rogers YH, Blazej RG, Champe M, Pfeiffer BD, Wan KH, Doyle C, Baxter EG, Helt G, Nelson CR, Gabor GL, Abril JF, Agbayani A, An HJ, Andrews-Pfannkoch C, Baldwin D, Ballew RM, Basu A, Baxendale J, Bayraktaroglu L, Beasley EM, Beeson KY, Benos PV, Berman BP, Bhandari D, Bolshakov S, Borkova D, Botchan MR, Bouck J, Brokstein P, Brottier P, Burtis KC, Busam DA, Butler H, Cadieu E, Center A, Chandra I, Cherry JM, Cawley S, Dahlke C, Davenport LB, Davies P, de Pablos B, Delcher A, Deng Z, Mays AD, Dew I, Dietz SM, Dodson K, Doup LE, Downes M, Dugan-Rocha S, Dunkov BC, Dunn P, Durbin KJ, Evangelista CC, Ferraz C, Ferriera S, Fleischmann W, Fosler C, Gabrielian AE, Garg NS, Gelbart WM, Glasser K, Glodek A, Gong F, Gorrell JH, Gu Z, Guan P, Harris M, Harris NL, Harvey D, Heiman TJ, Hernandez JR, Houck J, Hostin D, Houston KA, Howland TJ, Wei MH, Ibegwam C,

Jalali M, Kalush F, Karpen GH, Ke Z, Kennison JA, Ketchum KA, Kimmel BE, Kodira CD, Kraft C, Kravitz S, Kulp D, Lai Z, Lasko P, Lei Y, Levitsky AA, Li J, Li Z, Liang Y, Lin X, Liu X, Mattei B, McIntosh TC, McLeod MP, McPherson D, Merkulov G, Milshina NV, Mobarra C, Morris J, Moshrefi A, Mount SM, Moy M, Murphy B, Murphy L, Muzny DM, Nelson DL, Nelson DR, Nelson KA, Nixon K, Nusskern DR, Pacleb JM, Palazzolo M, Pittman GS, Pan S, Pollard J, Puri V, Reese MG, Reinert K, Remington K, Saunders RD, Scheeler F, Shen H, Shue BC, Siden-Kiamos I, Simpson M, Skupski MP, Smith T, Spier E, Spradling AC, Stapleton M, Strong R, Sun E, Svirskas R, Tector C, Turner R, Venter E, Wang AH, Wang X, Wang ZY, Wasarman DA, Weinstock GM, Weissbach J, Williams SM, Woodage T, Worley KC, Wu D, Yang S, Yao QA, Ye J, Yeh RF, Zaveri JS, Zhan M, Zhang G, Zhao Q, Zheng L, Zheng XH, Zhong FN, Zhong W, Zhou X, Zhu S, Zhu X, Smith HO, Gibbs RA, Myers EW, Rubin GM, Venter JC. 2000. The genome sequence of *Drosophila melanogaster*. *Science* 287:2185-2195.

Artavanis-Tsakonas S, Rand MD, Lake RJ. 1999. Notch signaling: cell fate control and signal integration in development. *Science* 284:770-776.

Bagutti C, Forro G, Ferralli J, Rubin B, Chiquet-Ehrismann R. 2003. The intracellular domain of teneurin-2 has a nuclear function and represses zic-1-mediated transcription. *J Cell Sci* 116:2957-2966.

Baker NE, Zitron AE. 1995. *Drosophila* eye development: Notch and Delta amplify a neurogenic pattern conferred on the morphogenetic furrow by scabrous. *Mech Dev* 49:173-189.

Baumgartner S, Martin D, Hagios C, Chiquet-Ehrismann R. 1994. Tenm, a *Drosophila* gene related to tenascin, is a new pair-rule gene. *EMBO J* 13:3728-3740.

Ben-Zur T, Feige E, Motro B, Wides R. 2000. The mammalian Odz gene family: homologs of a *Drosophila* pair-rule gene with expression implying distinct yet overlapping developmental roles. *Dev Biol* 217:107-120.

Brandau O, Schuster V, Weiss M, Hellbrand H, Fink FM, Kreczy A, Friedrich W, Strahm B, Niemeyer C, Belohradsky BH, Meindl A. 1999. Epstein-Barr virus-negative boys with non-Hodgkin lymphoma are mutated in the SH2D1A gene, as are patients with X-linked lymphoproliferative disease. *Hum Mol Genet* 8:2407-2413.

Chou TB, Perrimon N. 1996. The autosomal FLP-DFS technique for generating germline mosaics in *Drosophila melanogaster*. *Genetics* 144:1673-1679.

Cooper MTD, Bray SJ. 1999. Frizzled regulation of Notch signalling polarizes cell fate in the *Drosophila* eye. *Nature* 397:526-530.

Dgany O, Wides R. 2002. The *Drosophila* odz/ten-m gene encodes a type I, multi-

- ply cleaved heterodimeric transmembrane protein. *Biochem J* 363:633–643.
- Drabikowski K, Trzebiatowska A, Chiquet-Ehrismann R. 2005. *ten-1*, an essential gene for germ cell development, epidermal morphogenesis, gonad migration, and neuronal pathfinding in *Caenorhabditis elegans*. *Dev Biol* 282:27–38.
- Ellis MC, Weber U, Wiersdorff V, Mlodzik M. 1994. Confrontation of scabrous expressing and non-expressing cells is essential for normal ommatidial spacing in the *Drosophila* eye. *Development* 120:1959–1969.
- Fascetti N, Baumgartner S. 2002. Expression of *Drosophila* *Ten-a*, a dimeric receptor during embryonic development. *Mech Dev* 114:197–200.
- Feng K, Zhou XH, Oohashi T, Morgelin M, Lustig A, Hirakawa S, Ninomiya Y, Engel J, Rauch U, Fassler R. 2002. All four members of the *Ten-m/Odz* family of transmembrane proteins form dimers. *J Biol Chem* 277:26128–26135.
- Frankfort BJ, Nolo R, Zhang Z, Bellen H, Mardon G. 2001. Senseless repression of rough is required for R8 photoreceptor differentiation in the developing *Drosophila* eye. *Neuron* 32:403–414.
- Frankfort BJ, Pepple KL, Mamlouk M, Rose MF, Mardon G. 2004. Senseless is required for pupal retinal development in *Drosophila*. *Genesis* 38:182–194.
- Freeman M. 1998. Complexity of EGF receptor signalling revealed in *Drosophila*. *Curr Opin Genet Dev* 8:407–411.
- Herranz H, Stamatakis E, Feiguin F, Milan M. 2006. Self-refinement of Notch activity through the transmembrane protein *Crumbs*: modulation of gamma-secretase activity. *EMBO Rep* 7:297–302.
- Jarman AP, Sun Y, Jan LY, Jan YN. 1995. Role of the proneural gene, *atonal*, in formation of *Drosophila* chorodotonal organs and photoreceptors. *Development* 121:2019–2030.
- Kaufmann RC, Li S, Gallagher PA, Zhang J, Carthew RW. 1996. *Ras1* signaling and transcriptional competence in the R7 cell of *Drosophila*. *Genes Dev* 10:2167–2178.
- Lee JD, Treisman JE. 2001. The role of Wingless signaling in establishing the anteroposterior and dorsoventral axes of the eye disc. *Development* 128:1519–1529.
- Levine A, Gartenberg D, Yakov R, Lieberman Y, Budai-Hadrian O, Bashan-Ahrend A, Wides R. 1997a. The genetics and molecular structure of the *Drosophila* pair-rule gene *odd Oz* (*odz*). *Gene* 200:59–74.
- Levine A, Weiss C, Wides R. 1997b. Expression of the pair-rule gene *odd Oz* (*odz*) in imaginal tissues. *Dev Dyn* 209:1–14.
- Levine A, Bashan-Ahrend A, Budai-Hadrian O, Gartenberg D, Menasherow S, Wides R. 1994. *Odd Oz*: a novel *Drosophila* pair rule gene. *Cell* 77:587–598.
- Lossie AC, Nakamura H, Thomas SE, Justice MJ. 2005. Mutation of *17Rn3* shows that *Odz4* is required for mouse gastrulation. *Genetics* 169:285–299.
- Mieda M, Kikuchi Y, Hirate Y, Aoki M, Okamoto H. 1999. Compartmentalized expression of zebrafish *ten-m3* and *ten-m4*, homologues of the *Drosophila* *ten(m)/odd Oz* gene, in the central nervous system. *Mech Dev* 87:223–227.
- Minet AD, Rubin BP, Tucker RP, Baumgartner S, Chiquet-Ehrismann R. 1999. *Teneurin-1*, a vertebrate homologue of the *Drosophila* pair-rule gene *ten-m*, is a neuronal protein with a novel type of heparin-binding domain. *J Cell Sci* 112:2019–2032.
- Mollereau B, Domingos PM. 2005. Photoreceptor differentiation in *Drosophila*: from immature neurons to functional photoreceptors. *Dev Dyn* 232:585–592.
- Nunes SM, Ferralli J, Choi K, Brown-Luedi M, Minet AD, Chiquet-Ehrismann R. 2005. The intracellular domain of *teneurin-1* interacts with *MBD1* and *CAP/ponsin* resulting in subcellular codistribution and translocation to the nuclear matrix. *Exp Cell Res* 305:122–132.
- Oohashi T, Zhou XH, Feng K, Richter B, Morgelin M, Perez MT, Su WD, Chiquet-Ehrismann R, Rauch U, Fassler R. 1999. Mouse *ten-m/Odz* is a new family of dimeric type II transmembrane proteins expressed in many tissues. *J Cell Biol* 145:563–577.
- Otaki JM, Firestein S. 1999. *Neurestin*: putative transmembrane molecule implicated in neuronal development. *Dev Biol* 212:165–181.
- Pappu KS, Mardon G. 2004. Genetic control of retinal specification and determination in *Drosophila*. *Int J Dev Biol* 48:913–24.
- Rakovitsky N, Buganim Y, Swissa T, Kinel-Tahan Y, Cohen MA, Levine A, Wides R. *Drosophila Ten-a* is a maternal pair-rule and patterning gene. (Submitted).
- Ready DF, Hanson RE, Benzer S. 1976. Development of the *Drosophila* retina, a neurocrystalline lattice. *Dev Biol* 53:217–240.
- Rebay I, Fleming RJ, Fehon RG, Cherbas L, Cherbas P, Artavanis-Tsakonas S. 1991. Specific EGF repeats of Notch mediate interactions with *Delta* and *Serrate*: implications for Notch as a multifunctional receptor. *Cell* 67:687–699.
- Resino J, Salama-Cohen P, Garcia-Bellido A. 2002. Determining the role of patterned cell proliferation in the shape and size of the *Drosophila* wing. *Proc Natl Acad Sci U S A* 99:7502–7507.
- Rubin BP, Tucker RP, Martin D, Chiquet-Ehrismann R. 1999. *Teneurins*: a novel family of neuronal cell surface proteins in vertebrates, homologous to the *Drosophila* pair-rule gene product *Ten-m*. *Dev Biol* 216:195–209.
- Rubin BP, Tucker RP, Brown-Luedi M, Martin D, Chiquet-Ehrismann R. 2002. *Teneurin 2* is expressed by the neurons of the thalamofugal visual system in situ and promotes homophilic cell-cell adhesion in vitro. *Development* 129:4697–4705.
- Sundaram MV. 2005. The love-hate relationship between *Ras* and *Notch*. *Genes Dev* 19:1825–1839.
- Tomlinson A, Ready DF. 1987. Neuronal differentiation in the *Drosophila* ommatidium. *Dev Biol* 120:366–376.
- Tucker RP, Chiquet-Ehrismann R, Chevron MP, Martin D, Hall RJ, Rubin BP. 2001. *Teneurin-2* is expressed in tissues that regulate limb and somite pattern formation and is induced in vitro and in situ by *FGF8*. *Dev Dyn* 220:27–39.
- Voas MG, Rebay I. 2004. Signal integration during development: insights from the *Drosophila* eye. *Dev Dyn* 229:162–175.
- Wang XZ, Kuroda M, Sok J, Batchvarova N, Kimmel R, Chung P, Zinszner H, Ron D. 1998. Identification of novel stress-induced genes downstream of *chop*. *EMBO J* 17:3619–3630.
- Wieschaus E, Nusslein-Volhard C. 1986. Looking at embryos. In: Roberts DB, editor. *Drosophila: a practical approach*. Washington, DC: IRL Press. p 199–227.
- Wilson R, Ainscough R, Anderson K, Baynes C, Berks M, Bonfield J, Burton J, Connell M, Cosey T, Cooper J, et al. 1994. 2.2 Mb of contiguous nucleotide sequence from chromosome III of *C. elegans*. *Nature* 368:32–38.
- Wolff T, Ready DF. 1993. Pattern formation in the *Drosophila* retina. In: Bate M, Martinez Arias A, editors. *The development of Drosophila melanogaster*. Plainview, NY: Cold Spring Harbor Press. p 1277–1325.
- Yang L, Baker NE. 2006. Notch activity opposes *ras*-induced differentiation during the second mitotic wave of the developing *Drosophila* eye. *BMC Dev Biol* 6:8.
- Zhou XH, Brandau O, Feng K, Oohashi T, Ninomiya Y, Rauch U, Fassler R. 2003. The murine *Ten-m/Odz* genes show distinct but overlapping expression patterns during development and in adult brain. *Gene Expr Patterns* 3:397–405.